Biomacromol. J., Vol. 5, No. 2, 140-151, December 2019.

Biomacromolecular Journal
www.bmmj.org

Spectroscopic Studies on the Interaction of Gold Nanoparticles with Lysozyme

S. Mohammadi[a], K. Khajeh[b], M. Taghdir[a], N. Farahani[c] and B. Ranjbar[a,c,*]

[a]*Department of Biophysics, Faculty of Biological Sciences, Tarbiat Modares University, P. O. Box: 14115-175, Tehran, Iran*
[b]*Department of Biochemistry, Faculty of Biological Sciences, Tarbiat Modares University, P. O. Box: 14115-175, Tehran, Iran*
[c]*Department of Nanobiotechnology, Faculty of Biological Sciences, Tarbiat Modares University, P. O. Box: 14115-175, Tehran, Iran*

(Received 28 June 2020, Accepted 6 July 2020)

ABSTRACT

Gold nanoparticles are promising materials for biomedical applications because of the attractive optical properties such as the absorption and scattering of light at resonant wavelength. Due to the fruitful applications of gold nanoparticles (GNPs), they are appropriate for a variety of biological studies. One of the most important applications of nanoparticles is protein carriers, in which transport of therapeutically relevant protein is done to *in vivo* or *in vitro* targets. Protein folding and properties of probable intermediates during the folding of proteins had been investigated in several studies. The molten globule state, a main intermediate of protein folding, has native-like secondary but perturbation of tertiary structure. Consequently, the influence of gold nanoparticles concentration on a model protein was studied by far- and near-UV circular dichroism (CD), Fourier transform infrared spectroscopy (FTIR), UV-Vis spectroscopy, dynamic light scattering (DLS), transmission electron microscopy (TEM), intrinsic fluorescence emission spectroscopy and 8-Anilino-1-naphthalenesulfonic acid binding. The results indicated that the interactions between gold nanoparticles and lysozyme lead to the formation of molten globule-like state.

Abbreviations: Hen egg white lysozyme (HEWL); Circular dichroism (CD); 8-Anilino-1-naphthalenesulfonic acid (ANS); Dynamic light scattering (DLS); Transmission electron microscopy (TEM); Gold nanoparticles (GNPs); Fourier transform infrared (FTIR)

Keywords: Gold nanoparticles, Molten globule-like state, Lysozyme, Circular dichroism

INTRODUCTION

The chemical and physical properties of matter are powerfully directed by the extent and kind of the electronic motion when electrons are confined to a nanometer scale. Consequently, conversion of the materials size to nanoscopic dimensions leads to the appearance of unique and novel properties which are compared to bulk material [1]. Nanoparticles have large surface to volume ratio because they range normally between 1 and 100 nm. Due to their large surface volume ratio, nanoparticles demonstrate considerable adsorptive nature therefore they are suitable for binding with probes, chemical compounds, drugs and proteins [2].

Gold nanoparticles are promising materials for biomedical applications because of the attractive optical properties such as the absorption and scattering of light at resonant wavelength. This localized surface plasmon resonance phenomenon is the creator of the ruby red color of conventional gold colloids. The use of gold for in vitro and in vivo applications has generally been favored by the bioinert nature and nonreactive of this metal [1,3]. Because of useful applications of gold nanoparticles, they are appropriate for a variety of biological studies [4,5]. Nanoparticles based on gold chemistry can be used in a selection of biomedical applications in radiotherapy development, highly sensitive analytical assessments, thermotherapy, biosensors, molecular imaging and also drug and gene delivery [6-13]. Protein carriers are one of the most important applications of nanoparticles which consist of transport of therapeutically relevant protein to *in vivo* or *in vitro* targets. But it should be noted that in protein carriers, the protein structure can be altered by the interaction between protein and nanoparticles. The

*Corresponding author. E-mail: ranjbarb@modares.ac.ir

formation of molten globule might be as a result of changes in protein carriers.

The folding of a polypeptide chain into a special three-dimensional structure which is mainly specified by amino acid sequence is the ultimate process in protein synthesis, and also there is a partially folded intermediate state in protein folding [14-17]. Even though the two-state model is generally sufficient to analyze the denaturation method of small globular proteins [18,19], equilibrium intermediate structures have been seen with characteristics of the native and denatured states. These intermediates are more compact than the denatured state. They also have the interesting feature of keeping a native-like secondary structure content but perturbation of tertiary structure with a high increase of the intramolecular movement [15,19]. This state is called the molten globule state because of these physical specifications [19,20]. As the interaction of a chiral molecule with polarized light is extremely special, circular dichroism is a much useful technique to observe any induced conformational change in the macromolecular structure [21-24]. Molten globule-like state was distinguished from other states as study of secondary and tertiary structure by far- and near-UV circular dichroism (CD) spectroscopy, respectively.

Several studies have indicated the molten globule state of various proteins in different conditions, such as the acid-induced unfolding of wild type Escherichia coli 5-enolpyruvylshikimate 3-phosphate synthase (EPSPS) and its three different variants (G96A, A183T and G96A/A183T) [23], acid denaturation of aspergillus niger glucoamylase [24], bacillus licheniformis α-amylase at low pH induced by 1,1,1,3,3,3-hexafluoroisopropanol [25], p53 in the presence of Hsp90 [26], and human serum albumin (HSA) in the presence of 3-β-hydroxybutyrate [27]. Also there are many studies on the effect of nanoparticles on proteins in recent years. N. Ajdari and *et al*. investigated gold nanoparticle interactions in human blood by thromboelastography and showed prothrombogenic effects, and reduction in R values in a concentration dependent manner [28]. W. Lai and *et al*. studied on the protein corona formed from human plasma on 20 nm silver and gold nanoparticles and demonstrated that all nanoparticles obtained negative charges after interacting with plasma [29]. When Lysozyme or β-lactoglobulin adsorbed onto silica nanoparticles result in a rapid change in protein conformation [31,32]. Bovine serum albumin (BSA) can be used to identify the role of nanoparticles on protein structure because of conformational changes of it at different pH range [31].

In this paper, the interaction of gold nanoparticles with a model protein is investigated. Hen egg white lysozyme (HEWL) that is a compact globular protein with 129 residues consisting of a three-stranded antiparallel β-sheet, five α-helices, and a large amount of β-turn and random coil [33,34] was employed as a model protein. Four disulfide bonds with most of the cysteine residues located in the α-helices stabilize its structure [34]. This enzyme is an alkaline molecule (isoelectric point = 11.35) and has antitumor, antiviral, antifungal, and immune modulatory activities [35]. The adsorption of this enzyme on surfaces has been investigated, and little tendency for structural alterations upon surface adsorption has been reported [36]. Results of protein adsorption research indicated that the major driving force is hydrophobicity or electrostatics. Although hydrophobic interactions drive the adsorption of lysozyme on polymeric surfaces [38,39], the adsorption on inorganic materials is mainly because of electrostatic nature [40,41]. The adsorption of lysozyme on silica nanoparticles shows a great loss of α-helix content at wide surface coverage [41]. The adsorption of this enzyme on gold nanorods indicates a slight variation in the longitudinal surface plasmon resonance intensity and under these conditions, the thermodynamic stability of the enzyme increases without any considerable change in conformation [4,43]. In this study, we produced a molten globule-like state of lysozyme with the adsorption of enzyme on spherical gold nanoparticles. The molten globule-like state in lysozyme has been characterized by far- and near-UV circular dichroism (CD), FTIR spectroscopy, UV-Vis spectroscopy, dynamic light scattering (DLS), transmission electron microscopy (TEM), intrinsic fluorescence emission spectroscopy and 8-Anilino-1-naphthalenesulfonic acid (ANS) binding.

MATERIALS AND METHODS

Chemicals

Hen egg white lysozyme (HEWL) was purchased from

Sigma (United States) and used without more purification. Trisodium citrate dihydrate, sodium borohydride ($NaBH_4$), tetrachloroauric(III) acid trihydrate ($HAuCl_4.3H_2O$), hexadecyltrimethylammonium bromide(CTAB), ascorbic acid, 8-anilino-1-naphthalenesulfonic acid (ANS) were purchased from Sigma. Potassium phosphate monobasic (potassium dihydrogen phosphate) KH_2PO_4 and potassium phosphate dibasic (dipotassium hydrogen phosphate) K_2HPO_4 were procured from Carlo Erba (Spain). During the experiments, all solutions were prepared in distilled water and filtered through a 0.22 μm membrane prior to use. Glasswares were absolutely cleared with dilute sulfo chromic acid/detergent solution and rinsed with distilled water before the experiments. The pH of the solutions was measured by pH meter (827 pH lab, Metrohm, Swiss made). The solutions were stirred by hotplate stirrer (labtech daihan labtech co., LTD).

Synthesis of Spherical Gold Nanoparticles

In this study, spherical gold nanoparticles were synthesized by the seed-mediated growth method [43]. The following procedure was started with preparation of small gold nanoparticles to be used as seeds. In the first step, three solutions were prepared as follows: (1) $HAuCl_4.3H_2O$ (0.01 M), (2) trisodium citrate dihydrate (0.01 M), $NaBH_4$ (0.04 M) solutions. Afterwards, 250 μl of 0.01 M solution of $HAuCl_4.3H_2O$ was added to 9750 μl of deionized water and then 250 μl of 0.01 M trisodium citrate dihydrate and 75 μl of 0.04 M $NaBH_4$ solutions were added respectively. The reaction mixture was stirred for 10 min. In the second step, 250 μl of 0.01 M $HAuCl_4.3H_2O$ was added in 9750 μl of 0.08 M CTAB. Then, 500 μl of 0.10 M ascorbic acid was added to solution, followed by addition of 1 ml of the seed solution. The reaction mixture was stirred for 10 min.

Characterization of Gold Nanoparticles

Formation of spherical gold nanoparticles was characterized by UV-Vis spectrophotometer (Cary 100) and transmission electronmicroscopy (TEM) (Zeiss-EM10C-80 KV). The absorption spectra of gold nanoparticles were recorded in the 400-700 nm wavelength range. Prior to imaging by TEM, sample was purified, re-dispersion in deionized water and ultrasonicated by a Misonix-S3000 sonicator. Diluted sample was drop-casted on formvar carbon coated grid and kept undisturbed for solvent evaporation.

Purification of Gold Nanoparticles

Gold nanoparticles were made in the presence of extra value of hexadecyltrimethyl-ammonium bromide (CTAB) as a cationic surfactant. Samples were purified with two rounds of centrifugation at 14,000 rpm for 10 minutes in centrifuge (Sigma 3-18KS) because of removing excess CTAB and separating unreacted gold ions from the solution. The first round supernatant was elutriated and gold nanoparticles sample was diluted by deionized water; but in the second round dilution was made with phosphate buffer (20 mM) to keep pH of the solution at 6.2. Gold nanoparticles were sonicated for 10 minutes at 25 °C due to dispersion before use.

Gold Nanoparticle-lysozyme Interaction

Stock solution of lysozyme (517 μM) was prepared in potassium phosphate buffer (20 mM, pH 6.2). A fixed concentration of the protein (10 μM) was treated with 4.8, 9.6, 14.4, 19.2, 24, 28.8, 33.6, 38.4 and 43.2 nM of purified GNPs. The samples were incubated at room temperature for 2-hours. Longer incubation time did not significantly affect the interaction between GNPs and lysozyme.

Circular Dichroism Spectropolarimetry

The interaction of a chiral molecule with polarized light is extremely exceptional and therefore this property can be utilized as a main technique to monitor macromolecular structures. Any conformational changes in the structure of macromolecules could be evaluated by circular dichroism [20]. Circular dichroism (CD) measurements were carried out by a Jasco J-715 spectropolarimeter to monitor possible changes in lysozyme conformation with different gold nanoparticles concentrations. All spectra were recorded at room temperature. The final spectra were calculated by subtracting the reference spectrum from the native protein spectrum. The results were reported in terms of molar ellipticity [θ] that is based on the average amino acid residue weight (MRW), as denoted below:

$$[\theta] = \frac{\theta \times 100 MRW}{cl}$$

where, c is the protein concentration in mg ml^{-1}, l is the light path length in centimeters and θ is the measured ellipticity in degrees at wavelength λ.

Fourier Transform Infrared (FTIR) Spectroscopy

All samples of lysozyme and lysozyme-nanoparticle complex were prepared and dried by lyophilizer (LYSFME-Snijders scientific) before FTIR measurements. These spectra were recorded on a Nicolet IR 100 (FTIR) and reported in the range of 400-4000 cm^{-1}.

Dynamic Light Scattering

Dynamic light scattering (DLS) is the most useful technique for measuring size distributions, in situ the sizes, and in some cases the shapes of nanoparticles in liquids [44]. The time-dependent oscillations in the intensity of scattered light that happens because of Brownian motion of particles in the suspension is measured by DLS. Analysis of these intensity oscillations permits the establishment of a correlation function to characterize the diffusion coefficient of particles. Afterwards, this diffusion coefficient was converted into a hydrodynamic diameter of the particles [45]. The hydrodynamic diameter of GNPs was measured by DLS (Zetasizer Nano series, Malvern). Particles size was expressed as hydrodynamic diameter and polydispersity index (PDI), which displays the size distribution of nanoparticles. PDI was recorded simultaneously with particle size measurement. Surface charge of GNPs was recorded from zeta potential measurement by DLS. Prior to DLS measurement, each sample was filtered through a 0.22 μm membrane to remove any dust particles.

Fluorescence Spectroscopy

The biochemical applications of fluorescence mostly include investigation of intrinsic protein fluorescence. Tyrosine, tryptophan, and phenylalanine residues are known to be fluorescent. An attractive feature of intrinsic protein fluorescence is the great sensitivity of tryptophan residue to its local environment. In response to conformational transitions, subunit association, substrate binding, or denaturation happen variations in the emission spectra of tryptophan. Externally added quenchers or nearby groups within the proteins have been reported to quench tryptophan [46]. Fluorescence measurements were carried out using a Perkin Elmer LS55 fluorescence spectrometer. The excitation wavelength was set at 280 nm and the emission spectra were recorded between 300 and 500 nm. All experiments were carried out at 25 °C.

ANS Fluorescence Spectroscopy

8-Anilino-1-naphthalenesulfonic acid (ANS) binding experiments were performed using a Perkin Elmer LS55 fluorescence spectrometer. The ANS emission was scanned between 400 and 600 nm with an excitation wavelength of 380 nm.

RESULTS AND DISCUSSION

Characterization of Spherical Gold Nanoparticles

Formation of spherical gold nanoparticles was monitored by transmission electron microscopy and UV-Vis spectroscopy. The surface plasmon resonance absorption band of gold nanoparticle appeared in the visible region at 525 nm [5,48]. The spectra of gold nanoparticles (Fig. 1) showed an absorption band which could be referred to as the plasmon resonance absorption band, being characteristic of the spherical morphology of gold nanoparticles (Fig. 1). These results are consistent with previous studies, in which the absorption maximum of gold nanoparticles was depended on the shape and size of the particles. The plasmon band maximum typically falls between 520 and 530 nm for spherical gold nanoparticles [48]. Size and concentration of the GNPs were analyzed by TEM and atomic absorption spectroscopy, respectively. The average diameter of GNPs was 20 nm (Fig. 1).

Determination of Spherical Gold Nanoparticles Concentration

The average number of gold atoms per nanoparticle can be calculated from TEM analysis. The average diameters of the particles (D) were measured. The average number of gold atoms (N) for nanosphere was calculated by the following equation,

$$N = \frac{\pi \rho D^3}{6M}$$

where ρ is the density of gold (19.3 g cm^{-3}) and M is atomic

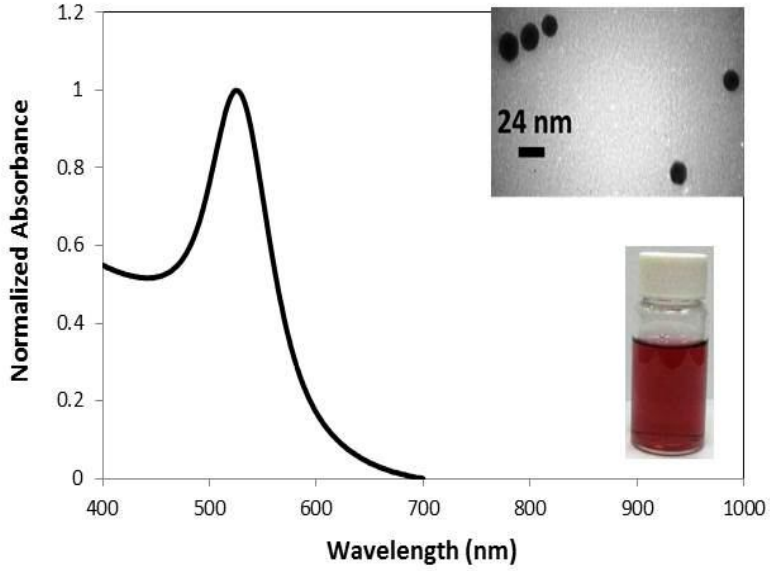

Fig. 1. UV-Vis spectrum of GNPs. The insets depict TEM image of the purified GNPs and the synthesized gold nanoparticles sample.

weight of gold (197 g mol^{-1}).

The molar concentration of gold nanosphere solution was calculated by dividing the total number of gold atoms N_{total}, (the initial amount of gold salt added to the reaction solution) over the average number of gold atoms per nanosphere (N) according to the following equation,

$$C = \frac{N_{Total}}{NVN_A}$$

where V is the volume of the solution in liter and N_A is the Avogadro's constant [49].

Dynamic Light Scattering Measurements

Dynamic light scattering was carried out to compare the size, polydispersity index (PDI), and zeta potential of GNPs before and after interaction with lysozyme (Table 1). The concentration of the lysozyme (10 μM) was treated with 24 nM of purified GNPs. Samples were dispersed in 20 mM potassium phosphate buffer, pH 6.2 and incubated at room temperature for 2-hours. Results in Table 1 show that size of GNPs is slightly larger after interaction with lysozyme. Therefore, the increase of lysozyme did not lead to increase of GNPs size. Polydispersity index (PDI) represents size distribution of colloidal nanoparticles. It is worth mentioning that compared to GNPs size, the PDI values of GNPs are a little smaller after interaction with lysozyme. It suggests that the sample is more polydispersed or heterogeneous particles prior to interaction with lysozyme. Notably, interacted lysozyme with gold nanoparticles significantly increased the magnitude of zeta potential, that it explains their improved non-covalent bond.

Circular Dichroism Studies

Circular dichroism spectroscopy in the far-UV spectral region (190-250 nm) determines the protein secondary structure. Within the specified wavelength range, the signal arises when the absorbing group (the peptide bond) is located in a regular and folded environment [22,50]. General structural changes of lysozyme (10 μM) in the presence and absence of different concentrations of purified GNPs (0-43.2 nM) were studied by far- and near-UV CD spectroscopy (Figs. 2 and 3). In far-UV CD region, concentration dependent changes of the molar ellipticity at 222 nm are shown in Fig. 2. The characteristic bands of α-helical structure at 222 nm show a slight increase in the presence of GNPs. The CD spectrum of a protein in the near-UV spectral region (250-320 nm) can characterize

Table 1. Gold Nanoparticles Dispersed in 20 mM Phosphate Buffer, pH 6.2

	Gold nanoparticle size (nm)	Polydispersity index	Zeta potential (mV)
Before interaction with lysozyme	28.06 ± 0.02	0.27 ± 0.01	2.96 ± 0.27
After interaction with lysozyme	30.93 ± 1.19	0.26 ± 0.01	11.15 ± 0.85

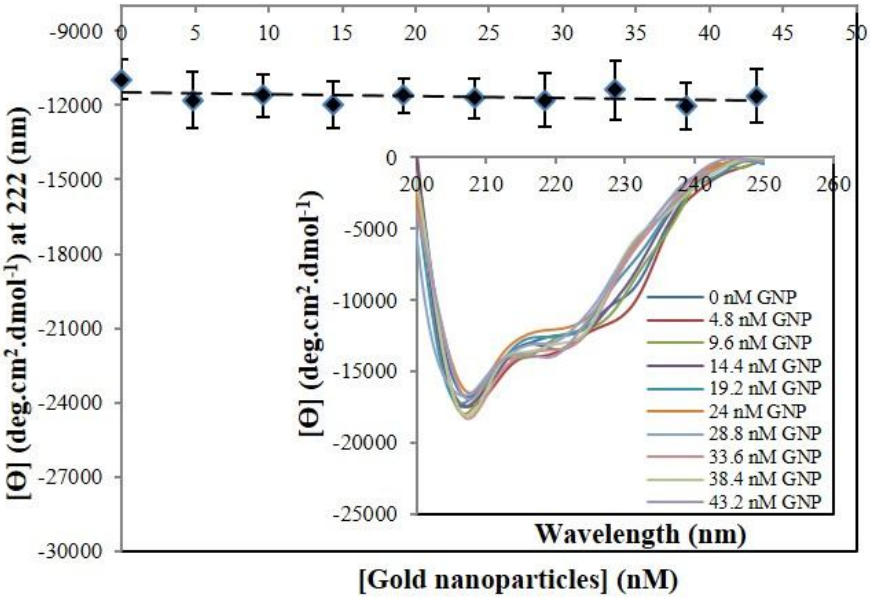

Fig. 2. Far-UV CD spectra of lysozyme in the presence and absence of GNPs. Concentration dependent variations of GNPs have been shown at 222 nm. The inset displays far-UV CD spectra of lysozyme in the presence of varying concentrations of purified GNPs.

certain aspects of tertiary structure. At these wavelengths, the aromatic amino acids are chromophores and each of them tends to have a special wavelength profile [22,51].

In near-UV CD region, concentration dependent changes of the molar ellipticity at 290 nm are represented in Fig. 3. The characteristic bands of tertiary structure content at 290 nm that are related to indole group of tryptophan residues in lysozyme (100 μM) demonstrate a significant decline in the presence of GNPs. Due to the obtained results from far- and near-UV CD spectroscopy that show a slight increase in helical content and a rigidity decrease in structure of lysozyme in the presence of different concentrations of GNPs confirm the formation of molten globule-like state of lysozyme.

Fourier Transform Infrared (FTIR) Spectroscopy Measurements

Fourier transform infrared spectra of lysozyme in the presence and absence of GNPs has been displayed in Fig. 4. The peptide group has 9 characteristic bands that amide I and II become visible as two main bands in the infrared spectrum. The amide I band in the 1600-1700 cm^{-1} region is mainly associated with C=O stretching vibration which coupled to the bending of the N-H bond and the

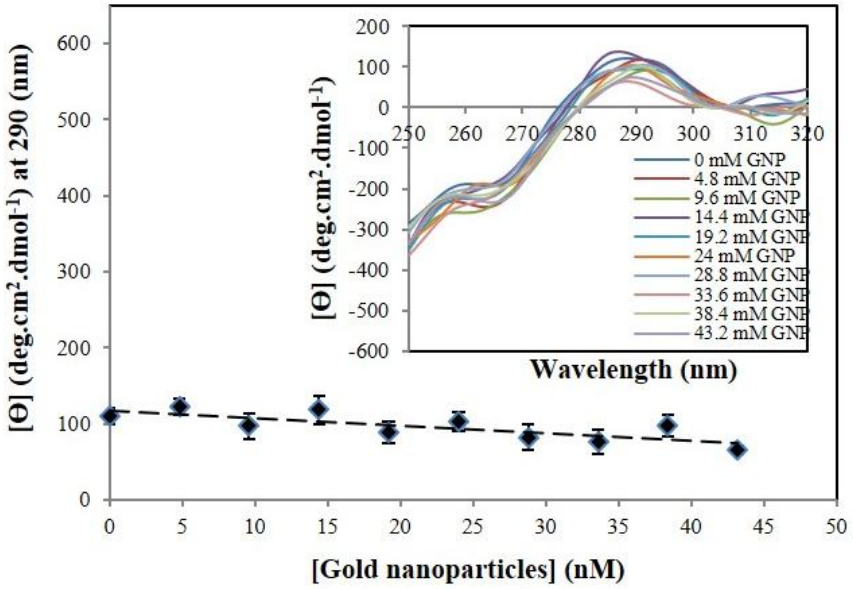

Fig. 3. Near-UV CD spectra of lysozyme in the presence and absence of GNPs. Concentration dependent variations of GNPs have been shown at 290 nm. The inset displays near-UV CD spectra of lysozyme in the presence of varying concentrations of purified GNPs.

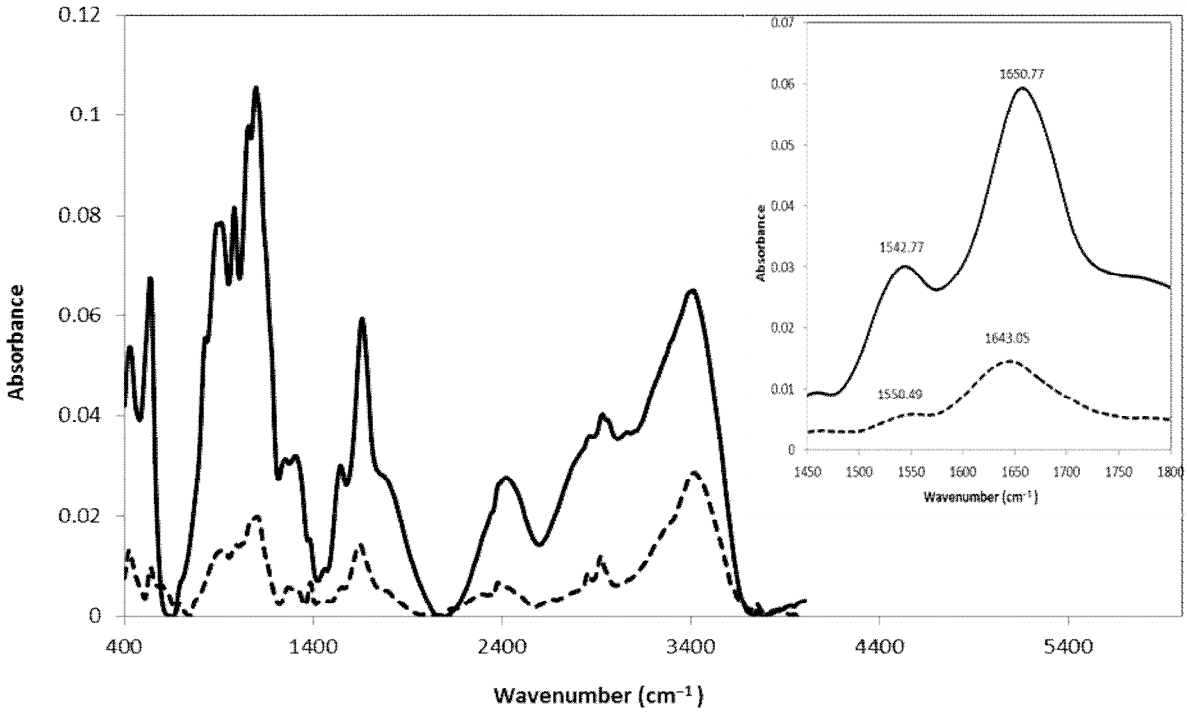

Fig. 4. FTIR spectra of lysozyme in 20 mM potassium phosphate buffer, pH 6.2. Free and GNPs treated samples of lysozyme are depicted by solid and dashed line, respectively. The inset displays magnified spectra in the amide I and amide II regions.

stretching of the C-N bond and also can be directly related to the backbone conformation of protein. The main agents responsible for conformational sensibility of amide bands include hydrogen bonding and the coupling between transition dipoles [52,53]. Potential energy for the amide II band in the 1500-1600 cm^{-1} region arises mainly from the N-H bending, moreover, it derives from C-N and C-C stretching vibrations. Study of the intensity changes in these characteristic regions give an idea about the probability of the adsorption of biomolecules and non-covalent bond [4,53].

Figure 4 shows the absorbance peaks in the amide II region from 1500 to 1600 cm^{-1} and in the amide I region from 1600-1700 cm^{-1} for free and GNPs treated samples of lysozyme in 20 mM potassium phosphate buffer, pH 6.2 and after incubation at room temperature for 2-hours. The spectrum in the amide II region represents a shift from 1542.77 to 1550.49 cm^{-1} with a loss of intensity that clearly shows adsorbed lysozyme on GNPs surface. Several secondary structural elements contribute in different regions of the amide I band: β-sheet in the 1620-1645 cm^{-1} region, random coil in the 1645-1652 cm^{-1} region, α-helix in the 1652-1662 cm^{-1} region, and turns in the 1662-1690 cm^{-1} region [4,54-56]. Figure 4 demonstrates that the spectrum in the amide I region represents a shift from 1650.77 to 1643.05 cm^{-1} with a loss of intensity. In the other words, gold nanoparticles treated lysozyme lose random coil content that it is probably converted to a small amount of α-helix and β-sheet structures. FTIR, far- and near-UV CD spectroscopy results can indicate that GNPs induce molten globule-like state in lysozyme.

Fluorescence Measurements

Phenylalanine shows a structured emission with a maximum near 282 nm. The emission of tyrosine in water happens at 303 nm which is relatively insensitive to solvent polarity. The emission maximum of tryptophan in water happens near 340 nm which is extremely dependent on polarity and local environment. Fluorescence of the protein is generally excited at the absorption maximum near 280 nm or at longer wavelengths. The absorption of proteins at 280 nm is due both tyrosine and tryptophan residues. At wavelengths longer than 295 nm, the absorption is due mainly to tryptophan. Tryptophan fluorescence can be selectively excited at 295-305 nm [46]. The influence of different concentrations of purified GNPs (0-48 nm) on conformational changes of lysozyme (10 μM) was investigated by intrinsic fluorescence studies for excitation at 280 nm (Fig. 5). The fluorescence intensity of lysozyme increased in the presence of 4.8 nM of purified GNPs, indicating that in the folded state, tryptophan residues interact with the side-chains that effectively quench the emission. It was demonstrated [57] that between tryptophan 28, 62, 63, 108, 111 and 123 in hen egg white lysozyme, the bulk of the fluorescence of lysozyme in the native state originated from tryptophan 62 and 108. Moreover, there is an interaction among tryptophan 108 and tryptophan 62 in that the energy transfer happens from tryptophan 108 to tryptophan 62. Notice that all of the tryptophan residues become equivalent upon denaturation and the interaction of tryptophan 108 and tryptophan 62 is eliminated, such that a fraction of absorbed energy which eventually achieves to tryptophan 62 declines and as a result the fluorescence quenching decreases [58]. The fluorescence intensity of lysozyme decreased in the presence of 9.6, 14.4, 19.2, 24, 28.8, 33.6, 38.4, 43.2 and 48 nM of purified GNPs (Fig. 5). As mentioned earlier, tryptophan 62 could be considered as a key chromophore to be quenched by external GNPs [4,57].

Figure 5 demonstrates that lysozyme is directed toward GNPs through the same location and GNPs react as external quencher. Accordingly, it could be suggested that when lysozyme comes to the proximity of GNPs, the rigidity of the protein slightly decreases at the location of tryptophan residues (as indicated by circular dichroism spectra). These results can confirm the formation of molten globule-like state of lysozyme.

ANS Fluorescence Studies

ANS fluorescence has been widely utilized to detect the formation of molten globule-like state in the folding pathways of various proteins. ANS is not fluorescent in aqueous solutions; nevertheless, binding to hydrophobic pockets on proteins enhance its emission intensity [25,59-60]. This property of ANS was used to study the interaction between lysozyme (10 μM) and varying concentrations of gold nanoparticles. All samples showed an increase in their ANS fluorescence intensity by raising the concentrations of

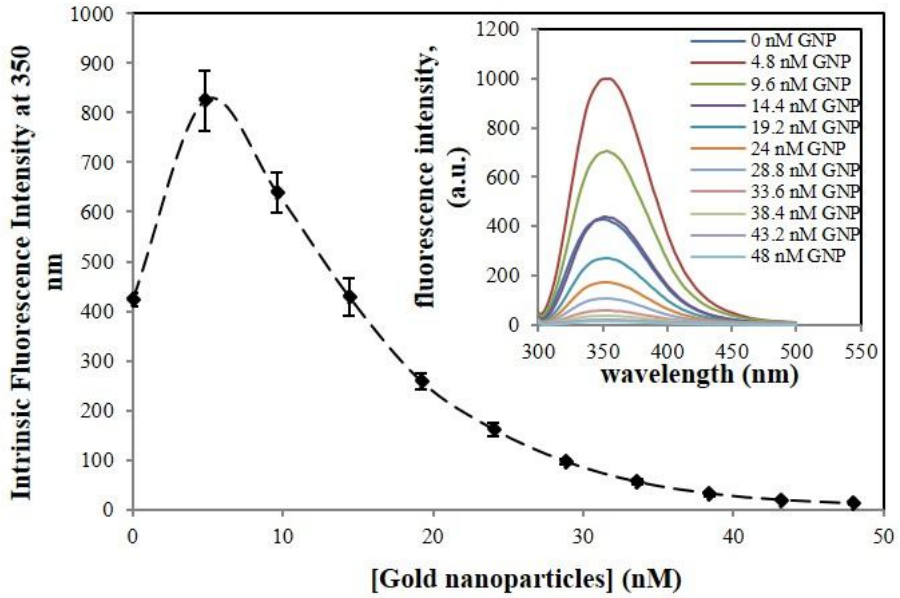

Fig. 5. Changes in intrinsic fluorescence of lysozyme in the presence of varying concentrations of purified GNPs at 350 nm. The inset displays intrinsic fluorescence of lysozyme in the presence of varying concentrations of purified GNPs. The excitation wavelength was 280 nm.

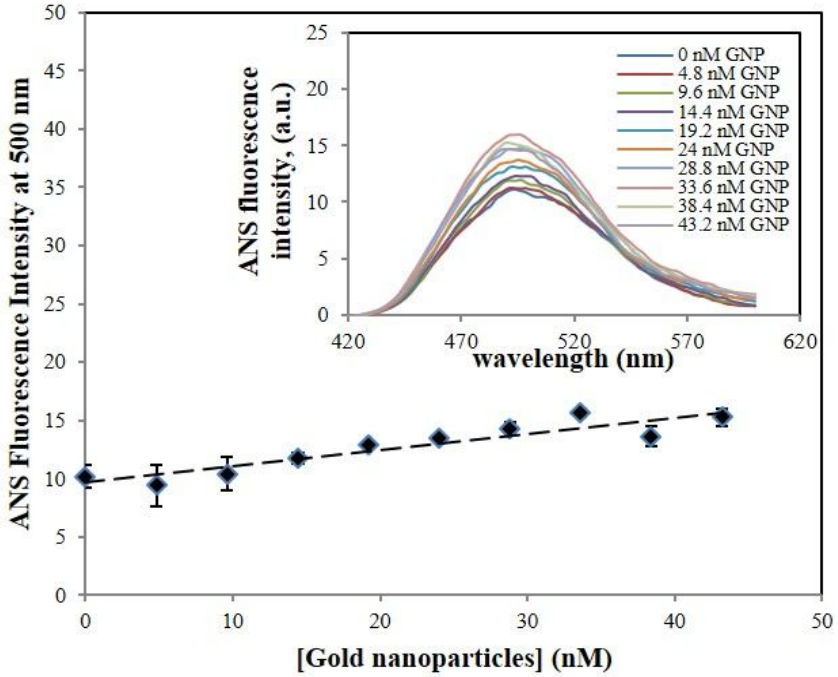

Fig. 6. Changes in ANS fluorescence of lysozyme in the presence of varying concentrations of purified GNPs at 500 nm. The inset displays ANS fluorescence of lysozyme in the presence of varying concentrations of purified GNPs. The excitation wavelength was 380 nm.

GNPs (Fig. 6). These findings indicate that lysozyme has more exposed hydrophobic patches in the presence of GNPs. Accordingly, ANS can bind to the exposed hydrophobic patches of lysozyme. The obtained results of ANS fluorescence demonstrate that the rigidity of lysozyme in the presence of GNPs decreases (as indicated by circular dichroism spectra). These results can confirm the results of intrinsic fluorescence and the formation of molten globule-like state of lysozyme.

CONCLUSIONS

The most recent researches in protein folding represent a variety of stages in protein unfolding and folding pathways. Under particular conditions, proteins can also illustrate a collapsed state with a partial order generally called molten globule state [25,61]. This state maintains the considerable secondary structure and is recognized by its hydrophobic dye-binding capacity, that is higher than that of the native and denatured states [23]. In this study, several biophysical methods were used to monitor the folding state and conformational changes of lysozyme (in 20 mM potassium phosphate buffer, pH 6.2) in the presence of varying concentrations of purified GNPs. We demonstrated the existence of an intermediate state in the presence of gold nanoparticles for lysozyme. The following results were acquired: (a) Far-UV CD spectra of lysozyme in the presence of gold nanoparticles indicates that helical content increases slightly. These results are in very good accord with maximum absorption bands observed at 1650.77 cm^{-1} in FTIR spectra. In near-UV CD region, the characteristic bands of tertiary structure content at 290 nm which are related to indole group of tryptophan residues in lysozyme demonstrate a significant decline in the presence of GNPs. Due to the obtained results from far- and near-UV CD spectroscopy that show a slight increase in helical content and a local decrease in tertiary structure of lysozyme in the presence of different concentrations of GNPs confirm the formation of molten globule-like state of lysozyme. (b) With regards to the intrinsic fluorescence of aromatic amino acid residues of lysozyme in the presence of gold nanoparticles, the rigidity of lysozyme decreases. These results indicate that there are changes in the tertiary structure of lysozyme in the presence of gold nanoparticles, resulting in exposure of the buried aromatic residues to polar solvents. (c) ANS fluorescence intensity increases with increment of concentration gold nanoparticles and the rigidity of lysozyme in the presence of GNPs decreases. These findings show that lysozyme in the presence of gold nanoparticles strongly bind to ANS and that can function as a special test for formation of the molten globule-like state. In summary, the combined results of far- and near-UV CD, fluorescence experiments, and Fourier transform infrared (FTIR) spectroscopy confirm the existence of molten globule-like state of lysozyme in the presence of different concentrations of GNPs. These results suggest the probability of utilizing gold nanoparticles as ideal nanocarrier candidates for drug delivery applications and appropriate ligands to study of molten globules.

ACKNOWLEDGMENTS

The authors would like to acknowledge financial support provided by Tarbiat Modares University.

REFERENCES

[1] Y. Xia, W. Li, C.M. Cobley, J. Chen, X. Xia, Q. Zhang, M. Yang, E.C. Cho, P.K. Brown, Acc. Chem. Res. 44 (2011) 914.

[2] R. Parveen, T.N. Shamsi, S. Fatima, Int. J. Biol. Macromol. 94 (2017) 386.

[3] B. Cárdenas, G. Sánchez-Obrero, R. Madueño, J.M. Sevilla, M. Blázquez, T. Pineda, J. Phys. Chem. C 118 (2014) 22274.

[4] T.T. Moghadam, B. Ranjbar, K. Khajeh, S.M. Etezad, K. Khalifeh, M.R. Ganjalikhany, Int. J. Biol. Macromol. 49 (2011) 629.

[5] X. Huang, S. Neretina, M.A. El□Sayed, Adv. Mater. 21 (2009) 4880.

[6] Y.-L. Chiu, T.M. Rana, Rna 9 (2003) 1034.

[7] J. Soutschek, A. Akinc, B. Bramlage, K. Charisse, R. Constien, M. Donoghue, S. Elbashir, A. Geick, P. Hadwiger, J. Harborth, Nature 432 (2004) 173.

[8] J.C.G. Jeynes, C. Jeynes, M.J. Merchant, K.J. Kirkby, Analyst 138 (2013) 7070.

[9] A.E. Prigodich, D.S. Seferos, M.D. Massich, D.A. Giljohann, B.C. Lane, C.A. Mirkin, ACS Nano 3

(2009) 2147.
[10] S. Dhar, W.L. Daniel, D.A. Giljohann, C.A. Mirkin, S.J. Lippard, J. Am. Chem. Soc. 131 (2009) 14652.
[11] H. Daraee, A. Eatemadi, E. Abbasi, S. Fekri Aval, M. Kouhi, A. Akbarzadeh, Artif. Cells, Nanomedicine, Biotechnol. 44 (2016) 410.
[12] C. Levinthal, J. Chem. Phys. 65 (1968) 44.
[13] Y. Kobashigawa, M. Demura, T. Koshiba, Y. Kumaki, K. Kuwajima, K. Nitta, Proteins Struct. Funct. Bioinforma. 40 (2000) 579.
[14] K. Kuwajima, K. Nitta, M. Yoneyama, S. Sugai, J. Mol. Biol. 106 (1976) 359.
[15] K. Kuwajima, J. Mol. Biol. 114 (1977) 241.
[16] P.L. Privalov, N.N. Khechinashvili, J. Mol. Biol. 86 (1974) 665.
[17] Y. Kuroda, S. Kidokoro, A. Wada, J. Mol. Biol. 223 (1992) 1139.
[18] M. Ohgushi, A. Wada, FEBS Lett. 164 (1983) 21.
[19] I. Protasevich, B. Ranjbar, V. Lobachov, A. Makarov, R. Gilli, C. Briand, D. Lafitte, J. Haiech, Biochemistry 36 (1997) 2017.
[20] B. Ranjbar, P. Gill, Chem. Biol. Drug Des. 74 (2009) 101.
[21] K. Khajeh, B. Ranjbar, H. Naderi-Manesh, A.E. Habibi, M. Nemat-Gorgani, Biochim. Biophys. Acta (BBA)-Protein Struct. Mol. Enzymol. 1548 (2001) 229.
[22] A. Nasiripourdori, H. Naderi-Manesh, B. Ranjbar, K. Khajeh, Int. J. Biol. Macromol. 44 (2009) 311.
[23] K. Haghani, K. Khajeh, A.H. Salmanian, B. Ranjbar, S. Bakhtiyari, Protein J. 30 (2011) 132.
[24] M.S. Zaroog, S. Tayyab, Process Biochem. 47 (2012) 775.
[25] A. Azizah, A. Halim, M.S. Zaroog, H.A. Kadir, S. Tayyab, Sci. World Journa 2014 (2014) 1.
[26] S.J. Park, B.N. Borin, M.A. Martinez-Yamout, H.J. Dyson, Nat. Struct. Mol. Biol. 18 (2011) 537.
[27] M. Bohlooli, A.A. Moosavi-Movahedi, F. Taghavi, M. Habibi-Rezaei, A. Seyedarabi, A.A. Saboury, F. Ahmad, Int. J. Biol. Macromol. 54 (2013) 258.
[28] N. Ajdari, C. Vyas, S.L. Bogan, B.A. Lwaleed, B.G. Cousins, Nanomedicine Nanotechnology, Biol. Med. 13 (2017) 1531.
[29] W. Lai, Q. Wang, L. Li, Z. Hu, J. Chen, Q. Fang, Colloids Surfaces B Biointerfaces 152 (2017) 317.
[30] X. Wu, G. Narsimhan, Biochim. Biophys. Acta (BBA)-Proteins Proteomics 1784 (2008) 1694.
[31] L. Shang, Y. Wang, J. Jiang, S. Dong, Langmuir 23 (2007) 2714.
[32] C.C.F. Blake, D.F. Koenig, G.A. Mair, A.C.T. North, D.C. Phillips, V.R. Sarma, Nature 206 (1965) 757.
[33] J.C. Cheetham, P.J. Artymiuk, D.C. Phillips, J. Mol. Biol. 224 (1992) 613.
[34] A.G. Murzin, S.E. Brenner, T. Hubbard, C. Chothia, J. Mol. Biol. 247 (1995) 536.
[35] Y.H. Samaranayake, L.P. Samaranayake, E.H.N. Pow, V.T. Beena, K.W.S. Yeung, J. Clin. Microbiol. 39 (2001) 3296.
[36] W. Norde, Colloids Surfaces B Biointerfaces 61 (2008) 1.
[37] S.Z. Qiao, H. Djojoputro, Q. Hu, G.Q. Lu, Prog. Solid State Chem. 34 (2006) 249.
[38] D. Shen, M. Huang, L.-M. Chow, M. Yang, Sensors Actuators B Chem. 77 (2001) 664.
[39] W. Norde, C. Haynes, J. Coll. Int. Sci. 169 (1994) 313.
[40] N. Shamim, H. Liang, K. Hidajat, M.S. Uddin, J. Colloid Interface Sci. 320 (2008) 15.
[41] A.A. Vertegel, R.W. Siegel, J.S. Dordick, Langmuir 20 (2004) 6800.
[42] T.T. Moghadam, B. Ranjbar, K. Khajeh, Int. J. Biol. Macromol. 51 (2012) 91.
[43] Z. Rezaei, B. Ranjbar, Eng. Life Sci. 17 (2017) 165.
[44] R. Pecora, J. nanoparticle Res. 2 (2000) 123.
[45] X.Z. Wang, L. Liu, R.F. Li, R.J. Tweedie, K. Primrose, J. Corbett, F.K. McNeil-Watson, Chem. Eng. Res. Des. 87 (2009) 874.
[46] T. Edition, Principles of Fluorescence Spectroscopy, Springer, 2006.
[47] W. Haiss, N.T.K. Thanh, J. Aveyard, D.G. Fernig, Anal. Chem. 79 (2007) 4215.
[48] N.A. Hatab, G. Eres, P.B. Hatzinger, B. Gu, J. Raman Spectrosc. 41 (2010) 1131.
[49] X. Liu, M. Atwater, J. Wang, Q. Huo, Colloids Surfaces B Biointerfaces 58 (2007) 3.
[50] S.M. Kelly, N.C. Price, Biochim. Biophys. Acta 1338 (1997) 161.
[51] S.M. Kelly, T.J. Jess, N.C. Price, Biochim. Biophys.

Acta (BBA)-Proteins Proteomics 1751 (2005) 119.
[52] J. Bandekar, Biochim. Biophys. Acta (BBA)-Protein Struct. Mol. Enzymol. 1120 (1992) 123.
[53] W.K. Surewicz, H.H. Mantsch, D. Chapman, Biochemistry 32 (1993) 389.
[54] S. Chakraborti, T. Chatterjee, P. Joshi, A. Poddar, B. Bhattacharyya, S.P. Singh, V. Gupta, P. Chakrabarti, Langmuir 26 (2009) 3506.
[55] S. Chakraborty, P. Joshi, V. Shanker, Z.A. Ansari, S. P. Singh, P. Chakrabarti, Langmuir 27 (2011) 7722.
[56] J.O. Speare, T.S. Rush, Biopolymers 72 (2003) 193.
[57] T. Imoto, L.S. Forster, J.A. Rupley, F. Tanaka, Proc. Natl. Acad. Sci. 69 (1972) 1151.
[58] K. Khalifeh, B. Ranjbar, K. Khajeh, H. Naderi-Manesh, M. Sadeghi, S. Gharavi, Biologia (Bratisl). 62 (2007) 258.
[59] Y. Goto, N. Takahashi, A.L. Fink, Biochemistry 29 (1990) 3480.
[60] S. Jagtap, M. Rao, J. Fluoresc. 19 (2009) 967.
[61] O.B. Ptitsyn, Adv. Protein Chem. 47 (1995) 83.